

# Production of woven aramid based protective equipment and improving its ballistic performance

DOI: 10.35530/IT.076.04.202462

ALİ ARI  
ÖZGÜR TEKASLAN

ZEHRA SEVER  
MEHMET KARAHAN

## ABSTRACT – REZUMAT

### Production of woven aramid based protective equipment and improving its ballistic performance

*In this study, various ballistic armour materials were designed using aramid fibre fabrics. Initially, soft armour designs were tested according to NIJ 0101.03 Level II standards across different configurations. However, the trauma depths observed in these tests exceeded the acceptable limits defined by the standards. To address this, a hard armour design was developed by incorporating reinforcement elements, such as silicon dioxide, graphene nanoplatelets, multi-walled carbon nanotubes, and  $Ti_3AlC_2$  (MAX phases) powders, into the aramid fabrics. These reinforcements were mixed with vinyl ester resin at concentrations of 3%, 5%, and 10%. The resulting mixture was impregnated into 25-layer aramid fabrics arranged in different orientations to produce composite plates. Ballistic tests were conducted on these plates in accordance with NIJ 0101.03 Level III standards. The tests revealed that the hybrid composite structure absorbed a substantial amount of energy, particularly in the central region of the plates. Plates reinforced with graphene nanoplatelets exhibited penetration under ballistic testing, but an improvement in ballistic performance was observed as the reinforcement density increased. Among all reinforcements, the best ballistic performance was achieved with  $Ti_3AlC_2$  (MAX phase) additives. As a result, prototype designs with enhanced protection levels and improved ballistic performance were successfully produced.*

**Keywords:** aramid fibres, protective equipment, ballistic performance, ballistic

### Producția de echipamente de protecție pe bază de țesături aramidice și îmbunătățirea performanței balistice a acestora

*În cadrul acestui studiu, au fost proiectate diverse materiale balistice pentru armuri utilizând țesături din fibre aramidice. Inițial, modelele de armuri moi au fost testate în conformitate cu standardele NIJ 0101.03 Nivel II în diferite configurații. Cu toate acestea, adâncimile traumatismelor observate în aceste teste au depășit limitele acceptabile definite de standarde. Pentru a remedia această problemă, a fost dezvoltat un model de armură rigidă prin încorporarea unor elemente de armare, precum dioxid de siliciu, nanoplăchete de grafen, nanotuburi de carbon cu pereți multipli și pulberi de  $Ti_3AlC_2$  (fază MAX) în țesăturile aramidice. Aceste elemente de armare au fost amestecate cu rășină vinilesterică în concentrații de 3%, 5% și 10%. Amestecul rezultat a fost impregnat în țesături aramidice cu 25 de straturi dispuse în diferite orientări pentru a produce plăci compozite. Testele balistice au fost efectuate pe aceste plăci în conformitate cu standardele NIJ 0101.03 Nivel III. Testele au arătat că structura compozită hibridă a absorbit o cantitate substanțială de energie, în special în zona centrală a plăcilor. Plăcile armate cu nanoplăchete de grafen au prezentat penetrare în timpul testelor balistice, dar s-a observat o îmbunătățire a performanței balistice odată cu creșterea densității armăturii. Dintre toate armăturile, cea mai bună performanță balistică a fost obținută cu aditivi  $Ti_3AlC_2$  (fază MAX). Prin urmare, au fost produse cu succes prototipuri cu niveluri de protecție sporite și performanță balistică îmbunătățită.*

**Cuvinte-cheie:** fibre aramidice, echipamente de protecție, performanță balistică, balistic

## INTRODUCTION

The defence industry is continuously evolving with advancements in engineering applications. The increasing sophistication of firepower and destructive systems has amplified the need for protection. In response, there is a demand for lightweight armour designs that do not compromise personnel mobility. Fibre-reinforced polymer composites have become key materials in advanced engineering applications due to their superior mechanical properties, such as high strength, stiffness, and low weight [1–4]. Furthermore, their adaptability to various shapes enables customisation to meet specific requirements.

The ballistic performance of an armour system is often defined in terms of its “energy absorption” capability [5–7]. Aramid fibre fabrics exhibit significantly higher ballistic performance compared to metallic materials. To further enhance energy absorption and achieve greater energy dissipation, various nano-fillers, such as graphene-based fillers, carbon nanotubes,  $SiO_2$ , and  $Ti_3AlC_2$ , are incorporated into the polymer matrix. These hybrid nanocomposites are a promising solution for engineering applications, offering improved performance in areas like ballistic protection while reducing cost and weight [8–10].

Several studies have been conducted to explore these advancements. For example, Cao et al. [11] investigated the ballistic capabilities of aramid fabrics impregnated with a shear-thickening fluid (STF) containing Pst-EA nanospheres at varying densities. They found that higher reinforcement density improved slip resistance by increasing friction between fabric threads, significantly enhancing the fabric's tear resistance. Similarly, Gao [12] studied the microstructure, mechanical properties, and fracture mechanisms of ceramic plates made from  $\text{Ti}_3\text{AlC}_2$  powders sintered at different temperatures and durations. Their results indicated that as the density of the plates increased, their strength and fracture toughness improved, with a 15% increase in fracture toughness observed. They concluded that  $\text{Ti}_3\text{AlC}_2$  powders could enhance energy absorption through increased strength and fracture toughness.

Costa et al. [13] designed and produced personal protective armour reinforced with graphene-based nano-pallents on aramid and jute fabrics. Their cost-benefit analysis revealed that hybrid nanocomposites could reduce armour weight and cost by 7% and 40%, respectively, without compromising performance. Xu et al. [14] examined the ballistic performance of two types of  $\text{B}_4\text{C}$  incorporated into an STF with  $\text{SiO}_2$ , producing samples with different combinations. Their ballistic tests showed that single-layer Twaron fabric treated with pure STF increased the ballistic limit velocity from 114 m/s to 160 m/s. Moreover, they found that a three-layer  $\text{B}_4\text{C}$ /STF/Twaron composite outperformed three layers of pure Twaron but was less effective than four layers of pure Twaron. An optimisation study demonstrated that placing one layer of  $\text{B}_4\text{C}$ /STF/Twaron composite in front of five layers of pure Twaron could improve overall ballistic resistance by 10% while maintaining similar areal density.

Divya et al. [15] used finite element modelling to compare the ballistic performance of carbon nanotubes (CNTs) and Kevlar fabrics under identical threat and boundary conditions. Their results showed that CNTs outperformed Kevlar, with significantly lower maximum deformation values, suggesting that CNTs should be more widely adopted in ballistic applications.

In this study, the ballistic performance of plates enhanced with carbon nanotubes, graphene,  $\text{SiO}_2$ , and  $\text{Ti}_3\text{AlC}_2$  (MAX phases) will be comprehensively

Table 1

MATERIALS USED IN THE PROJECT AND COMPANIES SUPPLIED	
Material	Company
Multi-Walled Carbon Nanotube	Nanograph
Silicone Dioxide ( $\text{SiO}_2$ ) Nanopowder	Nanograph
Graphene Nanoplatelet	Nanograph
$\text{Ti}_3\text{AlC}_2$ MAXene	Nano Chemazone
CT-709 Aramid	Teijin
CT 736 Aramid	Teijin
Vinylester	Composite market

evaluated at the NIJ Level III standard. The evaluation will involve CT 709 plain weave and CT 736 2×2 basket weave fabrics.

### MATERIALS AND METHODS

#### Material

In this study, the initial phase involved designing soft (unreinforced) armour using aramid fabrics with varying layer counts between 6 and 32. For this purpose, CT-709 and CT-736 aramid fabrics were cut to the required dimensions, and multiple designs were created based on the number of layers.

The study utilised four different reinforcement elements: Multi-Walled Carbon Nanotubes (MWCNTs), Graphene Nanoplatelets,  $\text{SiO}_2$  Nanopowder, and  $\text{Ti}_3\text{AlC}_2$  (MAX phases). CT-709 and CT-736 ballistic fabrics were incorporated, with Vinylester resin serving as the matrix material. Figure 1 illustrates the materials used in the scope of the project, while table 1 provides a list of the suppliers for the relevant materials.

Figure 1 presents the SEM images of the four reinforcement elements utilised in the project: Multi-Walled Carbon Nanotubes, Graphene Nanoplatelets,  $\text{SiO}_2$  Nanopowder, and  $\text{Ti}_3\text{AlC}_2$  (MAX phases). These SEM images were provided by the respective suppliers.

General properties of Aramid woven fabric CT 709 and CT 736 ballistic fabrics as reinforcement are given in table 2.

The properties of the fibres used in the preparation of reinforcement structures are given in table 3.

Close-up views of the Aramid woven fabrics used in the study are shown in figure 2.

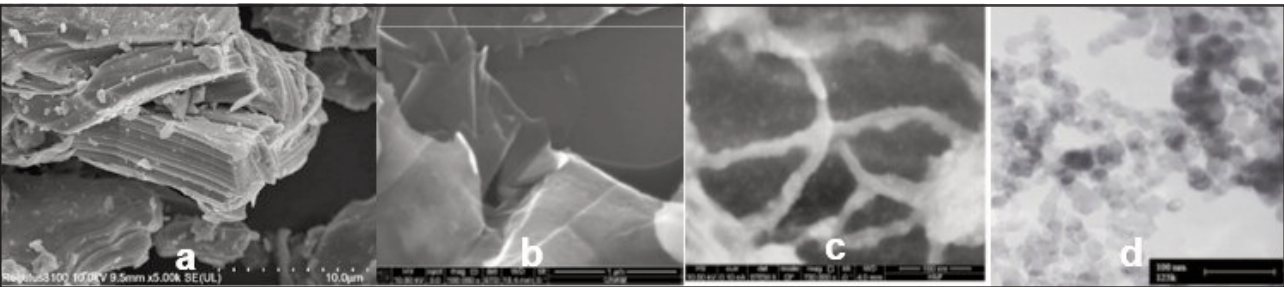


Fig. 1. SEM images of reinforcement elements purchased for use in ballistic armour production:  
a –  $\text{Ti}_3\text{AlC}_2$ ; b – Graphene Nanoplatelet; c – Multi-Walled Carbon Nanotube; d –  $\text{SiO}_2$

PROPERTIES OF ARAMID WOVEN FABRIC CT 709 AND CT 736 MATERIALS						
Reinforcement type	Knitting type	Warp/Fill direction of threads (0° – 90°)	Thread density (thread/10 cm)	Field density (g/m <sup>2</sup> )	Fold warp/fill (%)	Reinforcement thickness (mm)
Aramid woven fabric CT 709	Plain	Twaron 2000/ Twaron 2000	117/117	220	0.2/0.2	0.23
Aramid woven fabric CT 736	2*2 Basket weave	Twaron 2000/ Twaron 2000	336/336	410	0.8/0.8	0.6

Table 3

MECHANICAL PARAMETERS OF ARAMID FIBRES				
Fabric Name	Young's modulus (GPa)	Stress (cN/Tex)	Maximum elongation (%)	Density (g/cm <sup>3</sup> )
Twaron 2000	85	235	3.5	1.44

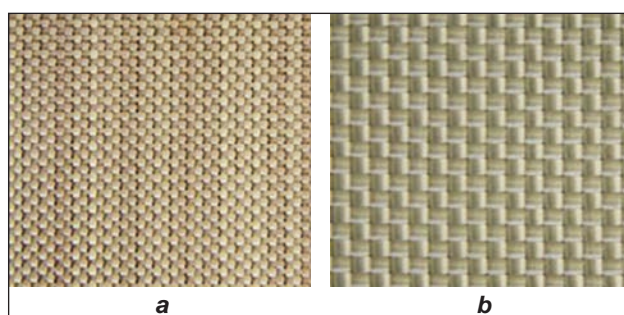


Fig. 2. Fabrics used in armour production: *a* – CT 709 Plain weaving; *b* – CT 736 2\*2 Basket weaving [16]

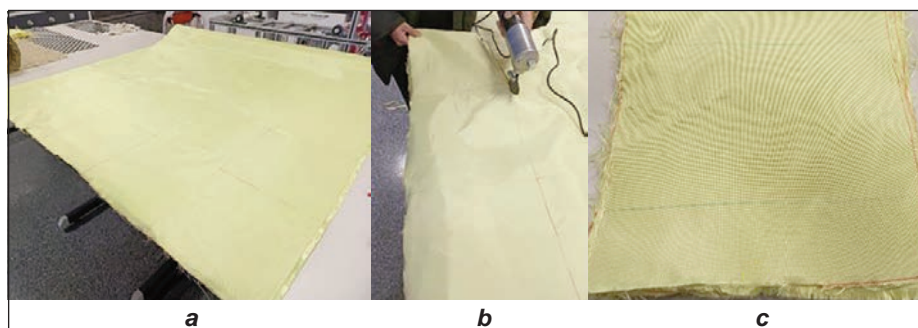


Fig. 3. Cutting stages of aramid fabrics: *a* – preparation of 30×30 cm dimensions; *b* – cutting with an aramid cutting knife; *c* – cutting fabrics

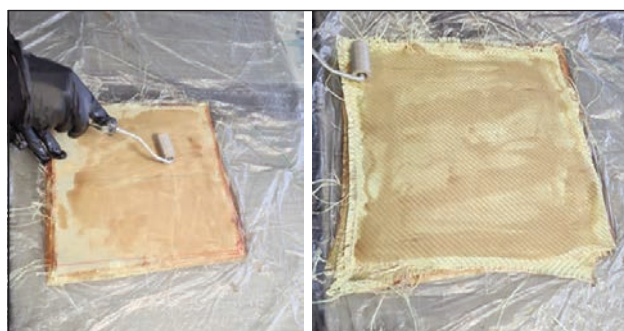


Fig. 4. The process of impregnating fabrics with resin by the hand-laying method

### Methods of production of reinforced composite armour

Ballistic fabrics were cut in 30 cm × 30 cm dimensions with an aramid fibre cutting knife, as shown in figure 3. Composite armour plates were fabricated using Al<sub>3</sub>C<sub>2</sub> reinforcements and vinylester resin, employing the hand-laying technique for layer-by-layer assembly (figure 4). Each plate consisted of a total of 25 layers: the first 10 layers were CT-709 fabric, followed by 5 layers of CT-736 fabric, and concluded with another 10 layers of CT-709 fabric. This hybrid composite structure was designed to maximise energy absorption by causing the projectile to change direction within the middle layers of the armour. A control sample (C0) was also produced without any reinforcement elements to serve as a baseline for comparison. During the production process, the hot press machine was preheated to 90°C, and the composite was pressed for 20 minutes under a pressure of 10 bar once the temperature was reached. After this, a rapid cooling process was applied for 10 minutes, maintaining the same pressure of 10 bar.

Following the impregnation of resin onto the fabric using the hand-laying method, the curing process was performed using a hot-pressing machine, as illustrated in figure 5. The hot press machine was preheated to 110°C, and the composite was subjected to a pressure of 10 bar for 60 minutes once the target

temperature was reached. Subsequently, a rapid cooling process was applied for 10 minutes while maintaining the same pressure of 10 bar. This process enhanced the adhesion between the resin and the fabric, resulting in improved composite integrity. The final samples produced are shown in figure 6. In this study, experimental factors and their corresponding levels were determined to evaluate their effects on the response variable, as outlined in table 4. By systematically altering the input variables, their impact on the response variable was analysed and interpreted in a structured manner.



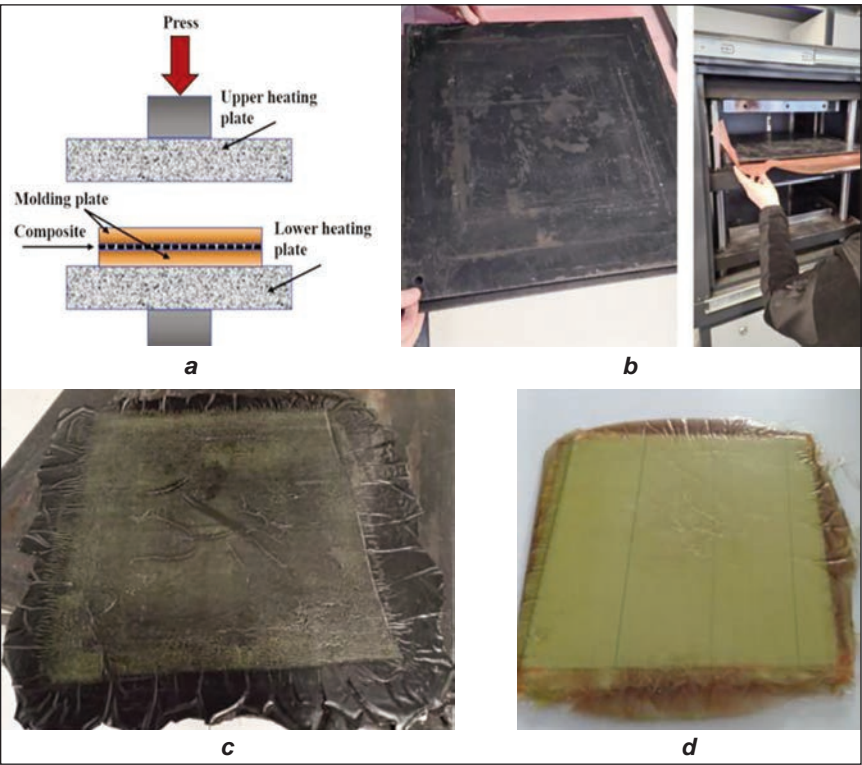


Fig. 5. Photos of: *a* – schematic picture of hot press; *b* – curing process of resin impregnated samples in hot press; *c* – sample with reinforcement added; *d* – sample without reinforcement element

distance, precisely 2.5 meters from the target. An MP5 pistol was employed during the trials. The bullets used in the tests had a core weight of 8 grams and a diameter of 9 mm, with a total weight of 12 grams, including the core, gunpowder, and cartridge. These bullets, all with a round nose and full metal jacket, were supplied by the Turkish Machinery and Chemical Industry Corporation. Bullet velocities were measured using a ProChrono model chrono-graph, based on photoelectric principles, manufactured by Competition Electronics Inc. After each shot, the velocity was displayed digitally on the device. As per NIJ standards, Type 1 Roman Plastilina (clay) was employed as the backing material. The clay was prepared in a box according to standard specifications. Targets were marked by placing tape on the front

Table 4

PROPERTIES OF THE COMPOSITE PLATES USED IN THIS STUDY			
Sample code	Reinforcement element	Reinforcement rate	Weight (g)
C0	-	0%	1300
C1	Graphene Nanoplatelet	3%	1325
C2	Graphene Nanoplatelet	5%	1349
C3	Graphene Nanoplatelet	10%	1351
C4	SiO <sub>2</sub> Nanopowder	3%	1344
C5	SiO <sub>2</sub> Nanopowder	5%	1344
C6	SiO <sub>2</sub> Nanopowder	10%	1348
C7	Ti <sub>3</sub> AlC <sub>2</sub>	3%	1367
C8	Ti <sub>3</sub> AlC <sub>2</sub>	5%	1369
C9	Ti <sub>3</sub> AlC <sub>2</sub>	10%	1371
C10	Multi Walled Carbon Nanotube	3%	1351
C11	Multi Walled Carbon Nanotube	5%	1356
C12	Multi Walled Carbon Nanotube	10%	1357

### Performing shooting tests

In the first phase of testing, a test apparatus conforming to NIJ 0101.03 Level II standards was utilised. The setup featured a 5-meter distance between the firearm's muzzle and the target. A velocity measurement device was positioned at the midpoint of this

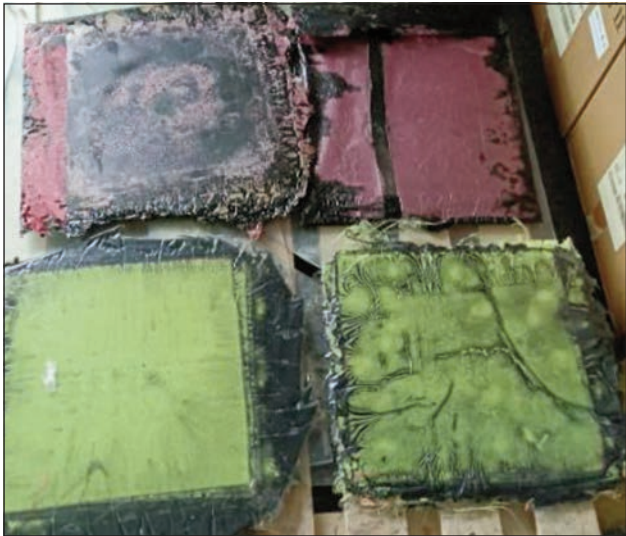


Fig. 6. Completed composite samples

surface of the panels. These tests were conducted at no cost at the Bursa Police College Shooting Range. In the second phase, ballistic tests adhered to NIJ 0101.03 Level III standards using the setup shown in figure 7. In this configuration, the distance between the firearm's muzzle and the target was 15 meters. A velocity measurement device was placed at the midpoint of the trajectory, 12 meters from the target. Full metal jacket (FMJ) bullets with a diameter of 7.62 mm, a length of 26.8 mm, and a weight of 9.7 grams were used. A bullet was classified as achieving full penetration if it either pierced through the panel completely or caused material displacement from the

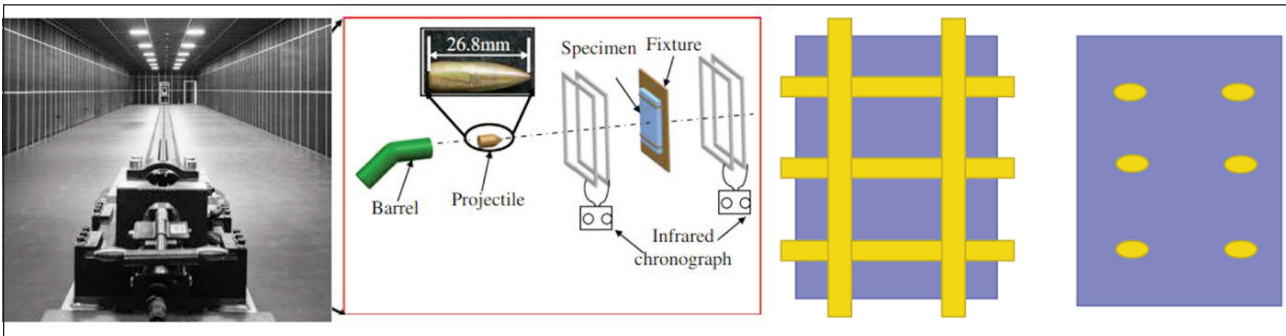


Fig. 7. Schematic illustration of the testing apparatus [17]



Fig. 8. Test setup and examples of tested samples

back of the panel. All other outcomes were recorded as partial penetration. The second-stage ballistic tests were conducted without charge at the NUROL Technology ballistic laboratories, as shown in figure 8. Firing tests were conducted in accordance with NIJ standards. A chronograph device was integrated into the test setup to measure muzzle velocity. The chronograph system included an initial photoelectric screen, a final photoelectric screen, and a data recording system. The tests utilised an OEHLER Research photoelectric display chronograph. Additionally, a test barrel approved by NIJ standards, capable of accommodating a barrel length of 56 cm and designed to withstand maximum pressure, was employed. To ensure accurate muzzle velocity measurements, the barrel was pre-heated by firing single shots prior to testing. The test firearm incorporated a firing mechanism compliant with the standards set by the American International Standards Institute (ANSI) and the Sporting Arms and Ammunition Manufacturer's Institute (SAAMI). The test setup also included a shooting stand that could accommodate barrels of various sizes and calibres, enabling precision firing. Muzzle velocity was calculated by averaging the highest partial penetration velocities and the

lowest full penetration velocities across an equal number of rounds, typically six shots per series. The projectile-armour interaction followed the mathematical principles of probability distribution, where the probability of penetration approaches zero at low speeds, approaches unity at high speeds, and increases progressively between these extremes as velocity increases. Table 5 provides the specifications of the ammunition used for NIJ Level II and Level III firing tests.

#### Determination of trauma depth and diameter

If the bullets do not penetrate the panels after firing, a trauma of a certain diameter and depth forms in the backing material. The depth of this trauma indicates the impact of the bullet on the back of the panel. Following each shot, the depth of the trauma was measured using a calliper with a precision of  $\pm 0.02$  mm. To better analyse the trauma geometry, a mould was prepared to replicate the trauma shape. During testing, the kinetic energy from the ballistic impact caused the flat-surfaced backing material positioned behind the ballistic test panel to deform. According to NIJ Level III standards, the maximum allowable depth for such deformation is 44 mm. The

Table 5

CHARACTERISTICS OF AMMUNITION USED FOR NIJ LEVEL II-III SHOTS AND MINIMUM ALLOWABLE CORE VELOCITY				
Protection level	Test ammunition	Nominal core weight (g)	Shot quantity	Minimum core speed (m/s)
II	MP5	8	6	367
III	7.62 308 Winchester FMJ	9.7	6	838

ballistic impact results in depressions and swelling on the flat surface of the clay backing layer. Accurate measurement of these depressions requires the use of a flat surface as a reference to ensure consistent and reliable results. For this reason, trauma values were determined by measuring from the highest point of the swelling to the lowest point of the depression, following this standardised approach. The depression depth encompasses the area from the region marked with dots in figure 8 to the bottom of the pit, even if it extends below the flat surface. Figure 9 illustrates how the depth of the trauma was measured after each shot.

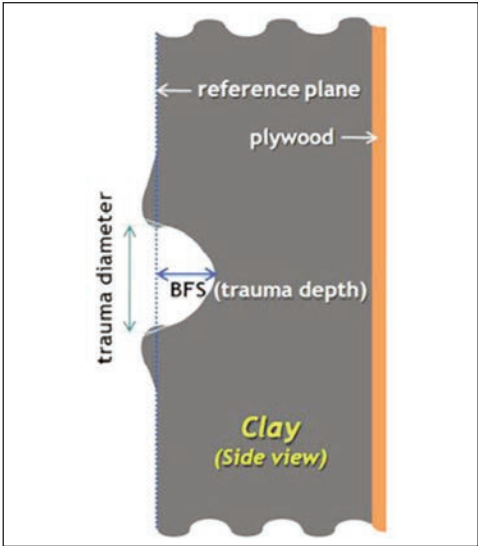


Fig. 9. Determination of trauma depth [17]

RESULTS AND DISCUSSION

When the results of the samples made with unreinforced aramid fabrics in NIJ 0101.03 Level II standards in the first stage were examined, it was seen that the trauma depth exceeded 44 mm. As a result, the 2nd stage was started. At this stage, the experiments were carried out using 7.62 mm FMJ ammunition in accordance with NIJ 0101.03 Level-III. Samples prepared using different reinforcement materials under the same conditions were tested on hot pressed plates. The muzzle velocity applied during the tests (838 m/sec  $\pm$ 15) was within the limits allowed by NIJ III rules.

Depth of trauma

The depth of the trauma occurring in the support material provides information about the ballistic resistance of the energy panels absorbed by the fabric layers. The depth of the trauma shows the effect of the lead energy transmitted behind the panel. If the panels spread the energy over a larger area, the volume of trauma will be lower. If the energy cannot spread over a wide area, a deeper and larger trauma will occur because the same amount of energy affects a smaller area [18, 19]. It is known that as the energy absorbed by the fabric layers increases, the depth and volume of trauma will decrease. It is

known that the number of fabric layers has the most significant effect on the depth of trauma, and the increase in the number of fabric layers is the most important parameter in reducing the depth of trauma. However, increasing the number of fabric layers also increases the panel weight. The average trauma depth in a 25-layer fabric was determined as 27.60 mm. In ballistic protection, panel weight should be taken into consideration as well as ballistic performance.

Ballistics and absorbed energies

During a ballistic impact, a shock wave is created in the ballistic plane due to the kinetic energy of the bullet. Some of this energy is absorbed by the fabric layers, and the rest is transmitted to the back of the panel, creating trauma. In panels that emit the energy wave at a higher speed, more energy is absorbed and less energy is transmitted to the back [20–22]. Trauma depth is very important because higher trauma depth causes bone fractures and internal organ bleeding. Therefore, when the panel stops a bullet, it will deform and its strength will decrease. In shooting tests, it was observed that the depth of trauma increased from the first shot to the sixth shot. Sample configurations and trauma depths performed in the first stage are given in Table 6. The produced samples were tested according to NIJ 0101.03 Level II standards. After the tests, the trauma depths exceeded 44 mm, outside the allowed limits. Since the samples did not meet the standards on the first or 2nd shot, no further shots were made. Therefore, the work continued by adding reinforcement elements to the plates.

Table 6		
LAYER THICKNESSES AND TRAUMA DEPTHS PREPARED IN THE STUDY		
Sample code	Number of floors	Trauma depth
S1	6	75
S2	8	72.8
S3	10	66.05
Q4	13	64.01
Q5	14	62.04
Q6	15	60.06
Q7	16	58.01
Q8	17	55.80
Q9	18	54.01
Q10	19	52.07
Q11	20	50.05
Q12	32	30.52

Table 7 shows the energy absorption performances of the samples performed in the second stage. The kinetic energy of the bullet is the energy that affects the panels. The produced samples were tested according to NIJ 0101.03 Level-III standards. Since the mass of the bullet is constant, the energy acting on the panels varies in proportion to the bullet



Table 7

NIJ III Test results			
Sample code	Average bullet speed (m/s)	Trauma depth (mm)	Energy absorbed by the panel ( $EA_{fabric}$ ) (J)
C0	850	pierced	-
C1	849	pierced	-
C2	857	pierced	-
C3	850	pierced	-
C4	849	pierced	-
C5	852	43	752
C6	851	41	795
C7	853	35	813
C8	848	31	846
C9	849	28	884
C10	858	27	871
C11	852	25	896
C12	848	21	973

speed. Since the bullet speed may vary within tolerances between shots, the energy affecting the panel varies from shot to shot.

The damage characteristics of the plates after firing according to NIJ 0101.03 Level-III are shown in table 7. There is only slight shear deformation and tensile deformation on the front surface of the non-punctured plates.

## RESULTS

In this study, various samples were tested for ballistic protection in accordance with NIJ 0101.03 Level II and NIJ 0101.03 Level -III standards. In this context, the results are stated below.

Soft ballistic designs have trauma depths greater than 44 mm. Thanks to the hybrid fabric structure in hard ballistic designs, a significant amount of energy is trapped in the middle part of the composite.

Graphene Nanoplatelet additive did not affect the trauma depth performance of the composite plate.

The sample (C4), produced with 3%  $SiO_2$  reinforcement, was drilled. However, when the reinforcement ratio is 5% (C5) and 10% (C6), the trauma depth is at the desired standards. In addition, it was observed that the absorbed energy values were very close to each other for these two samples.

MultiWalled Carbon Nanotube added samples showed the highest performance. As the nanotube's contribution rate increased, its ability to absorb energy on the plate increased, while the depth of trauma decreased.

Considering the amount of energy absorbed by nanotube reinforced C10 (3%) and C11 (5%) samples, while the C10 sample absorbed 25 J more energy than the C11 sample, the C12 (10%) sample absorbed 77 J more energy than the C11 sample.

The C12 sample absorbed 102 J more energy than the C10 sample.

When the weights are compared, the heaviest sample is Multi Walled Carbon. It was found to be Nanotube C12 (10%). However, since there is not a very high difference, it can be said that it is the sample with the highest ballistic performance.

When looking at trauma depths within the framework of standards, the lowest trauma depth is Multi Walled Carbon. The highest trauma depth was  $SiO_2$  when the nanotube belonged to the C12 (10%) sample. Nanopowder C5 (5%) is the sample. The trauma depth of the C5 sample is twice the trauma depth of the C12 sample.

When  $Ti_3AlC_2$  reinforced samples are compared among themselves, when the C8 (5%) and C9 (10%) samples were examined, it was seen that the C7 (3%) sample could absorb 33 J more energy than the C8 sample, and the C9 sample absorbed 38 J more energy than the C8 sample. However, the C9 sample was able to absorb 71 J more energy than the C7 sample. The reinforcement rate increased from 3% to 10%, but the ability to absorb energy increased by 46.47%.

We can list the performance of the reinforcement materials on the plate as follows: Carbon Nanotube >  $Ti_3AlC_2$  >  $SiO_2$  Nanopowder > Graphene Nanoplatelet.

## SUGGESTIONS

In this study, the ballistic efficiency of different reinforcement elements at different densities was examined by keeping the fabric coefficient constant. Looking at the results, it was seen that the best performance was obtained with Carbon Nanotubes. In this context, in terms of future studies, the ballistic efficiency of Carbon Nanotube reinforcement can be examined in different fabric layer numbers.

Lighter test samples with better ballistic performance can be obtained by changing the number of layers and reinforcement elements in different combinations.

The directions of the composite fabrics were kept constant within the scope of this study, and the effects of different orientations on ballistic performance can be examined.

## ACKNOWLEDGMENTS

We would like to express our gratitude to Bursa Technology Coordination and R&D Center (BUTEKOM) and Prof. Dr. Mehmet Karahan for providing infrastructure support for the realisation of this study.

This work was supported by the Research Fund of the OSTİM Technical University. Project Number: BAP 202223.

## REFERENCES

- [1] Haro, E.E., Szpunar, J.A., Odeshi, A.G., *Ballistic impact response of laminated hybrid materials made of 5086-H32 aluminum alloy, epoxy and Kevlar® fabrics impregnated with shear thickening fluid*, In: Composites Part A: Applied Science and Manufacturing, 2016, 87, 54–65
- [2] Lee, Y.S., Wetzel, E.D., Wagner, N.J., *The ballistic impact characteristics of Kevlar woven fabrics impregnated with a colloidal shear thickening fluid*, In: Journal of Materials Science, 2003, 38, 2825–2833
- [3] Grinevičiūtė, D., Abraitienė, A., Sankauskaitė, A., Tumėnienė, DM, Lenkauskaitė, L., Barauskas, R., *Influence of chemicals surface modification of woven fabrics on ballistic and stab protection of multilayer packets*, In: Materials Science, 2014, 20, 2, 193–197
- [4] Park, J.L., Yoon, B.I., Paik, J.G., Kang, T.J., *Ballistic performance of p-aramid fabrics impregnated with shear thickening fluid; Part I – Effect of laminating sequence*, In: Textile Research Journal, 2012, 82, 6, 527–541
- [5] Xu, Y.J., Zhang, H., Huang, G.Y., *Ballistic performance of B4C/STF/Twaron composite fabric*, In: Composite Structures, 2022, 279, 114754
- [6] Abedi, M.H., Eslami-Farsani, R., *Study on high velocity impact response of aramid fibres-epoxy / aluminum laminate composites toughened by ZrO<sub>2</sub> and SiO<sub>2</sub> nanoparticles*, In: Journal of Industrial Textiles, 2022, 51 (5\_suppl), 8175S–8195S
- [7] Yücel, T., *Ballistic Protective Elements Technology*, 2nd HIBM Command Publications, Kayseri, 1994
- [8] Bulut, H., *Use of Composite Materials in the Manufacturing of Ballistic Protective Equipment*, Master's Thesis, Istanbul Technical University, Institute of Science and Technology, Istanbul, 2003, 142994
- [9] Yumak, N., Pekbey, Y., Aslanta, K., *Investigation of Deformation Characteristics of Composite Materials Used in Armor Design*, In: Electronic Journal of Machinery Technologies, 2013, 10, 4, 1–21, 55
- [10] Xu, Y.J., Zhang, H., Huang, G.Y., *Ballistic performance of B4C/STF/ Twaron composite fabric*, In: Composite Structures, 2022, 279, 114754
- [11] Cao, S., Chen, Q., Wang, Y., Xuan, S., Jiang, W., Gong, X., *High strain -rate dynamic mechanical properties of Kevlar fabrics impregnated with shear thickening fluid*, In: Composites Part A: Applied Science and Manufacturing, 2017, 100, 161–169
- [12] Gao, L., Han, T., Guo, Z., Zhang, X., Pan, D., Zhou, S., Li, S., *Preparation and performance of MAX phase Ti<sub>3</sub>AlC<sub>2</sub> by in-situ reaction of Ti-Al-C system*, In: Advanced Powder Technology, 2020, 31, 8, 3533–3539
- [13] Costa, U.O., da Costa Garcia Filho, F., Gómez -del Río, T., Júnior, É.P.L., Monteiro, S.N., Nascimento, L.F.C., *Characterization and ballistic performance of hybrid jute and aramid reinforcing graphite nanoplatelets in high-density polyethylene nanocomposites*, In: Journal of Materials Research and Technology, 2024, 28, 1570–1583
- [14] Xu, Y.J., Zhang, H., Huang, G.Y., *Ballistic performance of B4C/STF/Twaron composite fabric*, In: Composite Structures, 2022, 279, 114754
- [15] Divya, S., Praveenkumar, S., Akthar, A.S., Karthiksundar, N., *Performance variation of graphene nanoplatelets reinforced concrete concerning dispersion time*, In: Materials Today: Proceedings, 2023
- [16] Ari, A., Karahan, M., *Relationship between elastic properties and energy absorption of different types of aramid and UHMWPE composites used in ballistic protection*, In: Industria Textila, 2024, 75, 4, 484–497, <https://doi.org/10.35530/it.075.04.2023137>
- [17] Ari, A., Karahan, M., Kopar, M., Ahrarı, M., *The effect of manufacturing parameters on various composite plates under ballistic impact*, In: Polymers and Polymer Composites, 2024, 30, <https://doi.org/10.1177/09673911221144874>
- [18] Karahan, M., Karahan, N., Ari, A., *The impact energy dissipation analysis of woven para-aramid fabrics*, In: AATCC Journal of Research, 2025, <https://doi.org/10.1177/24723444241288275>
- [19] Ari, A., Karahan, M., *The comparative analysis of energy dissipation behaviour of woven and UD para-aramid fabrics*, In: Industria Textila, 2024, 75, 5, 658–668, <https://doi.org/10.35530/IT.075.05.202470>
- [20] Ari, A., Karahan, M., Nasir, A., *Mechanical properties of aramid and UHMWPE thermoplastic composites: Numerical and experimental trials*, In: Industria Textila, 2024, 75, 5, 633–643, <https://doi.org/10.35530/IT.075.05.202410>
- [21] Karahan, M., Yildirim, K., *Low velocity impact behaviour of aramid and UHMWPE composites*, In: Fibres and Textiles in Eastern Europe, 2015, 23, 3, 111, 97–105, <https://doi.org/10.5604/12303666.1152522>
- [22] Khan, M.I., Umair, M., Hussain, R., Karahan, M., Nawab, Y., *Investigation of impact properties of para-aramid composites made with a thermoplastic-thermoset blend*, In: Journal of Thermoplastic Composite Materials, 2023, 36, 2, 866–866

### Authors:

ALİ ARI<sup>1</sup>, ÖZGÜR TEKASLAN<sup>1</sup>, ZEHRA SEVER<sup>1</sup>, MEHMET KARAHAN<sup>2,3</sup>

Department of Weapon Industry Technician, Vocational School of Higher Education, Ostim Technical University,  
06374, Ankara, Türkiye  
e-mail: ozgur.tekaslan@ostimteknik.edu.tr, zehra.sever@ostimteknik.edu.tr

<sup>2</sup>Vocational School of Technical Sciences, Bursa Uludag University, 16059, Bursa, Türkiye  
e-mail: mkarahan@uludag.edu.tr

<sup>3</sup>Butekom Inc., Demirtas Dumlupinar OSB District,  
2nd Cigdem Street No:1/4, 16245, Osmangazi, Bursa, Türkiye

### Corresponding author:

ALİ ARI  
e-mail: ali.ari@ostimteknik.edu.tr